DOE/SC-CM-17-003

U.S. DEPARTMENT OF ENERGY | Office of Science

FY 2017 Third Quarter Performance Metric: Implement and evaluate the impacts of water management on the hydrologic cycle in the ACME model

July 2017

DISCLAIMER

Contents

Figures

1.0 Product Definition

Human activities associated with water use, reservoir operations, and groundwater pumping can induce pronounced effects on water resources availability and streamflows. Postel et al. [1996] estimated that 26% of global evapotranspiration is associated with human activities, and 56% of spatially and temporally available global runoff is withdrawn from water bodies. Also, unsustainable groundwater depletion to supplement surface water supply is a widespread practice across the globe, so about a third of Earth's largest groundwater aquifers are being rapidly depleted by human consumption [Wada et al. 2012, 2014; Richey et al. 2015]. Recognizing the critical role of water in the Earth system, human activities such as irrigation, reservoir operations, and groundwater pumping have been represented in some land surface models. Modeling experiments with Earth system models informed by modeling of the socio-economic drivers of human activities are only emerging [Hejazi et al. 2015]. Two products of research are described here.

First, building on previous efforts to better understand and represent the human-natural system feedbacks, new development has been implemented in an integrated water model based on the Model for Scale-Adaptive River Transport (MOSART) [Li et al. 2013, 2015] coupled to a water management (WM) model [Voisin et al. 2013a&b] to represent groundwater use and return flow. Return flow refers to unconsumed water such as that withdrawn for thermoelectric power generation and then returned to the streams. Driven by runoff simulated by a climate model and spatially distributed sectoral withdrawal and consumptive water demands simulated by the Global Change Assessment Model (GCAM) [Hejazi et al. 2015], MOSART-WM was applied to the US to simulate the spatial redistribution of water resources and water deficit by water use and flow regulation [Voisin et al. 2017].

Second, MOSART-WM has been coupled with the ACME Land Model (ALM) as a new model feature to represent irrigation and water management in ACME. This new capability will enable ACME to more realistically simulate water-cycle processes in the Earth system and understand water availability and its natural and human drivers. Global simulations have been performed with ALM-MOSART-WM to evaluate the impacts of irrigation and reservoir operations on streamflow and reservoir storage.

Water supply deficit, which should be negligible over the historical period, is reduced in simulations that included groundwater use and return flow. This demonstrates that the new development in MOSART-WM provides a more realistic representation of water management. Simulations using the coupled ALM-MOSART-WM demonstrated successful coupling in the ACME framework and a new capability to address science questions related to the interactions between human and natural processes that influence the regional and global water cycles.

2.0 Product Documentation

In the integrated water model, MOSART-WM, river transport is simulated by MOSART while reservoir operations and flow regulation are simulated by WM. WM is a large-scale water management model [Voisin et al. 2013a] that allocates water demands and manages reservoir releases and storage. WM relies on generic operating rules that mimic monthly releases and storage patterns based on the objectives of the reservoirs. The reservoir model is coupled to MOSART, which routes the regulated flow

from reservoirs to downstream channels as well as the local runoff in the hillslope and tributaries within each grid cell. The GCAM irrigation and non-irrigation demand are used as inputs to MOSART-WM.

In the previous implementation described in Voisin et al. [2013a,b], MOSART-WM only considers consumptive demand, although in reality a significantly larger amount of water can be withdrawn for non-consumptive use such as water for cooling thermoelectric power plants that is returned to rivers. In addition, the model limits demands to be provided by the surface-water systems only, which tends to exaggerate water stress. In more recent developments, Voisin et al. [2017] have addressed the limitations of MOSART-WM by considering groundwater supply as well as distinguishing consumptive and withdrawal demands and the associated return flow. Representing return flow in MOSART-WM requires both withdrawals and consumptive use for both irrigation and non-irrigation sectors. These are provided by GCAM and allocated to groundwater and surface-water systems. The unconsumed water is returned to the grid cells where withdrawals are distributed.

In the offline implementation of MOSART-WM, runoff is provided by an offline land surface model simulation; irrigation and non-irrigation water demands are provided by an offline GCAM simulation. This implementation lacks consistency between the irrigation demand simulated by GCAM and that simulated by the land surface model due to differences in spatial and temporal scales, process representations, and land use-land cover used in the two models. For more realistic simulations of irrigation effects and water supply deficit, a one-way coupling of MOSART-WM with the ACME Land Model (ALM) has been implemented. During the crop growing season, ALM calculates the irrigation demand at 6am local time each day based on the soil moisture status [Leng et al. 2013]. Irrigation is applied at a uniform rate over a 6-hour period by adding it to the precipitation input to the ALM grids. The runoff and irrigation demand are passed from ALM to MOSART-WM through the flux coupler used in ACME. Water balance checks are implemented in ALM and MOSART-WM to ensure water conservation in the coupled model. This simple one-way coupling of ALM with MOSART-WM provides a framework for future implementations to allow groundwater use and return flow, and two-way coupling in which unmet demand is passed from MOSART-WM to ALM through the flux coupler to constrain irrigation water supply in ALM.

The new developments in MOSART-WM to account for groundwater use and return flow are used to understand their contrasting local effects: more available supply due to the use of both surface water and groundwater versus more stress due to the consideration of withdrawals in addition to consumptive demand. A benchmark simulation and three numerical experiments were performed to understand and quantify the relative impacts of accounting for groundwater use and consumptive versus withdrawal demands and the associated return flow.

3.0 Results

3.1 A brief description of MOSART-WM

In the integrated water model, MOSART-WM, river transport is simulated by MOSART while reservoir operations and flow regulation are simulated by WM. WM is a large-scale water management model [Voisin et al. 2013a] that allocates water demands and manages reservoir releases and storage. WM relies on generic operating rules that mimic monthly releases and storage patterns based on the objectives of the reservoirs. In WM, non-irrigation water demand is met before irrigation demand. When

applied to the conterminous US, WM simulates reservoir operations explicitly in 1848 reservoirs, which are classified by their primary use into four categories: flood control, irrigation, flood control with irrigation, and other uses. Reservoir releases are managed to supply water to dependent grid cells that cannot meet their demand with their local supply (i.e., runoff generated at the grid cells). The dependency database associates each dam with all the downstream grid cells that are within reach (100 km buffer) of the stream impounded by the dam. Monthly release and storage targets are pre-computed for each reservoir based on the long-term historical mean monthly natural inflow simulated by MOSART, water demand simulated by GCAM, and the reservoir storage characteristics and purpose. Actual releases are adjusted monthly to simulate inter-annual variability of the releases, and adjusted daily for spilling and meeting minimum flow requirements (environmental flow requires minimum release of 10% of mean monthly natural flow, which also constrains withdrawals). The reservoir model is coupled to MOSART, which routes the regulated flow from reservoirs to downstream channels as well as the local runoff in the hillslope and tributaries within each grid cell. The GCAM irrigation and non-irrigation demand are used as inputs to MOSART-WM.

3.2 New development in MOSART-WM to represent groundwater use and return flow

In the previous implementation described in Voisin et al. [2013a,b], MOSART-WM only considers consumptive demand although in reality a significantly larger amount of water can be withdrawn for non-consumptive use such as water for cooling of thermoelectric power plants that is returned to rivers. In addition, the model limits demands to be provided by the surface-water systems only, which tends to exaggerate water stress. More realistic representations of the sources of sectoral (irrigation and non-irrigation) water supply and accounting for return flow from non-consumptive use are important for improving modeling of the interactions between human activities and surface hydrology. Voisin et al. [2017] addressed the limitations of MOSART-WM by considering groundwater supply as well as distinguishing consumptive and withdrawal demands and the associated return flow. To track groundwater use explicitly, the model uses irrigation and non-irrigation water demands simulated by GCAM and partitioned each into surface and groundwater demands based on predefined fractions derived from observed historical county-based USGS data [Kenny et al. 2009]. The fractions are held constant over the historical simulation. Demands allocated to groundwater supply are assumed to be always met, similar to other large-scale groundwater modeling approaches [Döll et al. 2009, 2012; Biemans et al. 2011; Wada et al. 2011; Pokhrel et al. 2012], but surface water system supply deficit is allowed and calculated.

Representing return flow in MOSART-WM requires both withdrawals and consumptive use for both irrigation and non-irrigation sectors. These are provided by GCAM and allocated to groundwater and surface-water systems as specified by the ratio discussed above. At each time step, WM allocates local storage (runoff, baseflow, water in the main channel) from the surface-water system to meet non-irrigation withdrawal first, and then irrigation withdrawals. Any unmet demand is allocated to the reservoirs that the specific grid cell depends on, with the same sectoral priority. The potential sectoral return flow within the grid cell is the difference between sectoral withdrawals and consumptive use from both surface-water and groundwater systems. The actual groundwater return flow is simply equal to the potential return flow from groundwater allocation because the demand allocated to the groundwater system is always met. The actual surface-water return flow is the potential surface return flow adjusted by

the fraction of withdrawal that is actually met. The total sectoral return flow is the sum of both surface and groundwater sources.

The unconsumed water is returned to the grid cells where withdrawals are distributed. We assume that the return flow from the irrigation sector returns to the surface-water system, which causes a delay for the return flow to enter the main channel due to routing in the hillslope and tributaries. Return flow from non-irrigation use is added directly to the main channel of the grid cell. Grid cells that are downstream can benefit from the return flow only if they are crossed by that stream, or a reservoir can capture the return flow and redistribute it. However, groundwater aquifer recharge dynamics are not taken into consideration in this offline implementation of MOSART-WM driven by simulated runoff. Figure 1 illustrates the processes represented by MOSART-WM conceptually with the added groundwater use and return flow components.

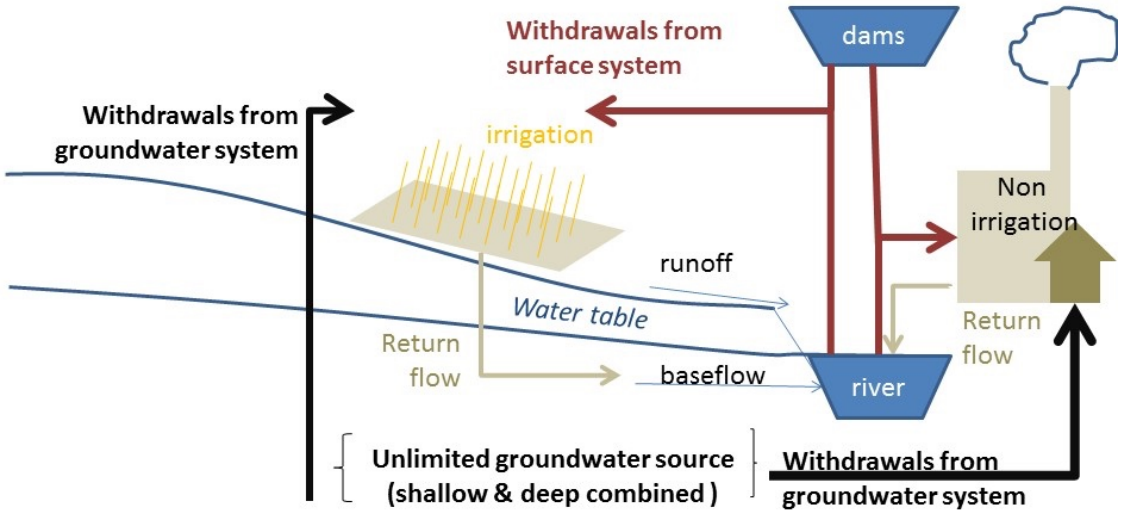

Figure 1. Conceptual diagram representing the interaction of the groundwater and return flow component within the integrated water model MOSART-WM. Irrigation and non-irrigation water is provided by both the surface-water sysem (red arrows) and groundwater system (black arrows). Return flow from both irrigation and non-irrigation water use (gray) is returned to the surface-water system only. Groundwater supply is assumed to be unlimited but unmet surface-water supply is tracked as surface-water deficit.

Figure 2a shows the fractions of demand assigned to the surface-water systems based on USGS data. There are large spatial variations across the US as driven by consumptive versus non-consumptive water use and availability of surface water. The ratio of total consumptive demand over the total withdrawal demand is shown in Figure 2b. It represents a spatially varying measure of the potential for return flow. Consumptive demands are 1/4 of the withdrawal demand on average over the US, 1/1.7 for irrigation and 1/10 for non-irrigation sectors. The ratio shown in Figure 1b has an east-west pattern that is related to the large withdrawals for the energy industry in the eastern US due to the widespread application of once-through cooling technology [Liu et al. 2015]. Figure 2c shows the total consumptive water demand in the US. High consumptive demand is in regions of intensive irrigation (the Great Plains, lower Mississippi, Columbia and Snake river valleys, over the Pacific Northwest, and Central Valley in California) and in regions of large urban centers. Comparing Figure 2a and 2c, the fraction of water demand assigned to groundwater source is larger (brown in Figure 2a) in regions with high irrigation demand in the Great Plains (the Ogallala Aquifer) and the Southeast and locally over the western US. Urban areas are also

groundwater dependent in the Midwest and the East Coast. The Upper Colorado and Missouri headwaters have little dependence on groundwater (blue strip in Figure 2a). Those regions should be less affected by groundwater use and return flow.

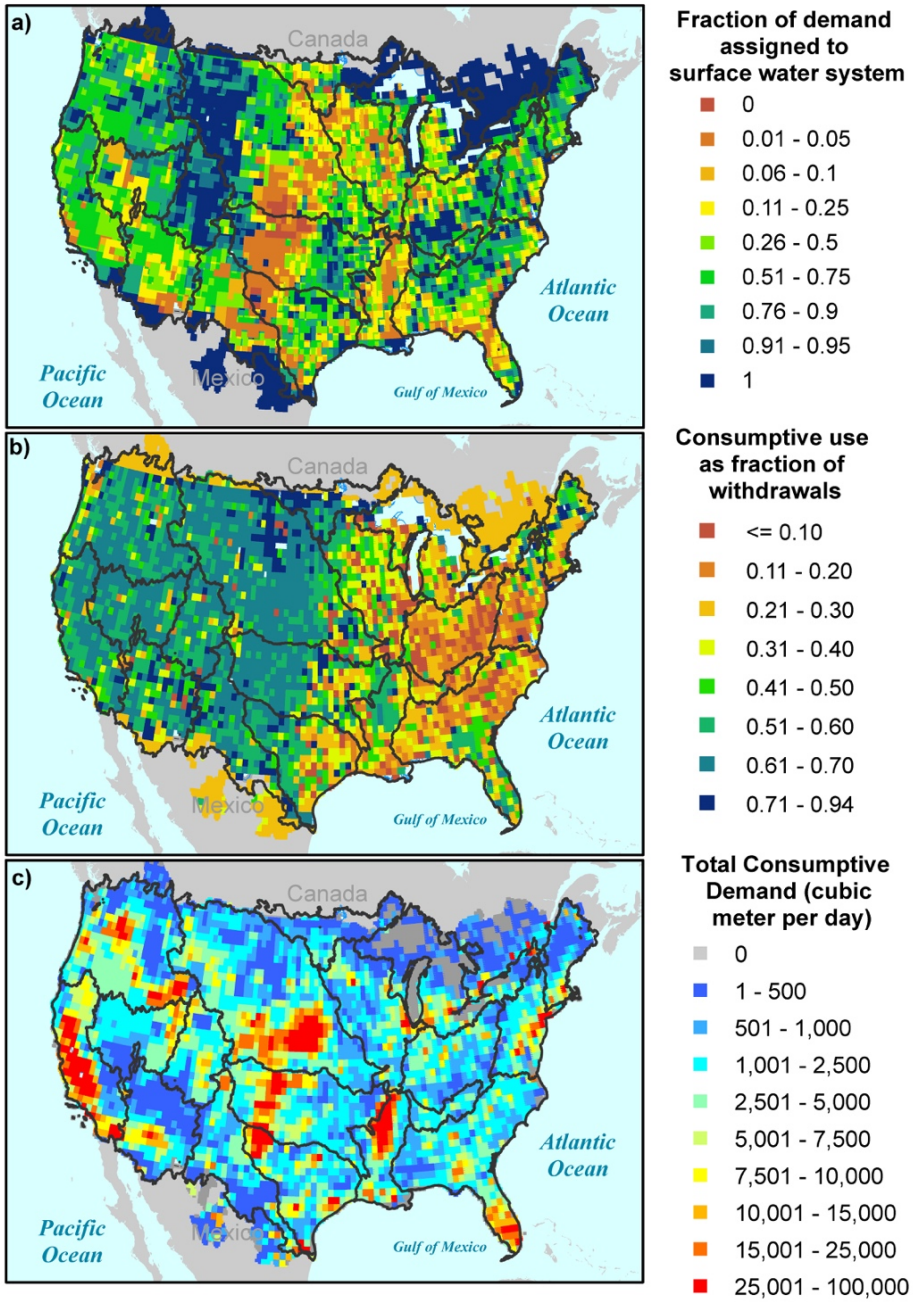

Figure 2. One-eigth-degree spatial distributions of (a) fraction of water demand assigned to the surface-water system based on Kenny et al. [2009], (b) consumptive water use as a fraction of the total water withdrawal, and (c) Total consumptive water demand in m3/day used as inputs to MOSART-WM.

3.3 Coupling of MOSART-WM with ALM

In the offline implementation of MOSART-WM described above, runoff is provided by an offline land surface model simulation and irrigation and non-irrigation water demands are provided by an offline GCAM simulation. This implementation lacks consistency between the irrigation demand simulated by GCAM and that simulated by the land surface model due to differences in spatial and temporal scales, process representations, and land use-land cover used in the two models. As the runoff input to MOSART is provided by the land surface model, which simulates irrigation demand different from that used in MOSART provided by GCAM, the offline implementation of MOSART-WM cannot fully represent the interactions between land surface hydrology, river transport, and flow regulations. For more realistic simulations of irrigation effects and water supply deficit, a one-way coupling of MOSART-WM with the ACME Land Model (ALM) has been implemented. As a proof of concept, groundwater use and return flow are not considered in the first demonstration described here.

During the crop growing season, ALM calculates the irrigation demand at 6am local time each day based on the soil moisture status [Leng et al. 2013]. Irrigation is applied at a uniform rate over a 6-hour period by adding it to the precipitation input to the ALM grids. The runoff and irrigation demand are passed from ALM to MOSART-WM through the flux coupler used in ACME. In MOSART-WM, irrigation demand is first subtracted from the local runoff. Irrigation demand not met by the local runoff is then withdrawn from the main channels regulated by the dams, and any remaining unmet demand is withdrawn directly from the reservoirs. Lastly, irrigation demand unmet by the reservoirs is recorded as supply deficit. Water balance checks are implemented in ALM and MOSART-WM to ensure water conservation in the coupled model. This simple one-way coupling of ALM with MOSART-WM provides a framework for future implementations to allow groundwater use and return flow, as described in the previous section, and two-way coupling in which unmet demand is passed from MOSART-WM to ALM through the flux coupler to constrain irrigation water supply in ALM.

3.4 Impacts of groundwater use and return flow

The new development in MOSART-WM to account for groundwater use and return flow can be used to understand their contrasting local effects: more available supply due to the use of both surface water and groundwater versus more stress due to the consideration of withdrawals in addition to consumptive demand. A benchmark simulation and three numerical experiments were performed to understand and quantify the relative impacts of accounting for groundwater use and consumptive versus withdrawal demands and the associated return flow. The benchmark simulation (denoted as WM) does not include groundwater use or return flow. The three experiments correspond to simulations with both groundwater use and return flow (WM_GW_return), groundwater use only (WM_GW), and return flow only (WM_return). The impacts are evaluated based on the simulated regulated flow and supply deficit at basin scale.

In the benchmark experiment, only consumptive demand is allocated to the surface-water system. A supply deficit occurs when the surface-water supply is below the consumptive demand. The supply deficit is simply equal to the difference between the demand and supply. In WM_return, the withdrawal demand (consumptive and non-consumptive) is allocated to the surface-water system only. If the surface-water supply is not sufficient to meet the withdrawal demand, the amount of water extracted, which is equal to the available surface-water supply, is made available for consumptive and non-consumptive uses in the

same ratio as the consumptive to non-consumptive demands. The water withdrawn for non-consumptive use is not available for any other allocation within the same simulation time step and is returned to the stream. In highly allocated basins, the supply deficit in GW_return may be higher than the supply deficit in the benchmark case because in the former, the total demand is higher and the deficit is proportionately distributed to the consumptive and non-consumptive uses, while in the latter, the demand (consumptive only) is lower and more easily met, especially in areas with low consumptive-to-withdrawal ratios (irrigation).

In WM_GW, the fraction of consumptive water demand allocated to the groundwater system is unconditionally met, but the fraction of consumptive water demand allocated to the surface-water system can be subjected to supply deficit depending on the surface-water availability. In WM_GW_return, the total consumptive and non-consumptive demand (i.e., withdrawal demand) is allocated to the groundwater and surface-water systems based on the same sectoral fraction as in WM_GW. The allocation to the surface-water system is subjected to supply deficit, which is distributed to consumptive and non-consumptive uses in the same ratio as the consumptive and non-consumptive demands in WM_return.

The differences among the four experiments can illustrate the individual and combined effects of groundwater use and return flow (i.e., water demand allocation, and sectoral water withdrawals and consumptive use), and how the hydrologic spatiotemporal patterns and water resources management (water supply deficit) respond specifically to return flow and groundwater use. The modeling framework is applied over the continental US at 1/8 degree resolution for the period of 1985-2004. Daily runoff was provided by an offline climate simulation and daily sectoral water demands were provided by an offline GCAM simulation downscaled to 1/8 degree resolution.

Meeting the historical water demand is an important metric for model performance of an integrated water model. The water demands simulated by GCAM represent well the water withdrawals reported by USGS in 1990 and 2005 with correlation coefficients of 77% and 87% respectively [Voisin et al. 2013b]. Therefore, a realistic model should simulate negligible water deficit over the historical period and an improvement in the representation of water management can be measured by a decrease in water supply deficit, if there was any. Figure 3 presents the change in relative supply deficit and therefore the ability to meet the historical water demand with the representation of groundwater use and return flow. The implementation of groundwater use and return flow improves the representation of water resources management, as measured by a decreased relative supply deficit. The South-Atlantic-Gulf, Ohio, and Upper Mississippi are the only regions with a slight increase in supply deficit with groundwater use and return flow due to uncertainty in allocation of demand to urban centers, uncertainty in the sources of supply (surface or groundwater), differences between withdrawals and consumptive uses, and uncertainty in the water management model.

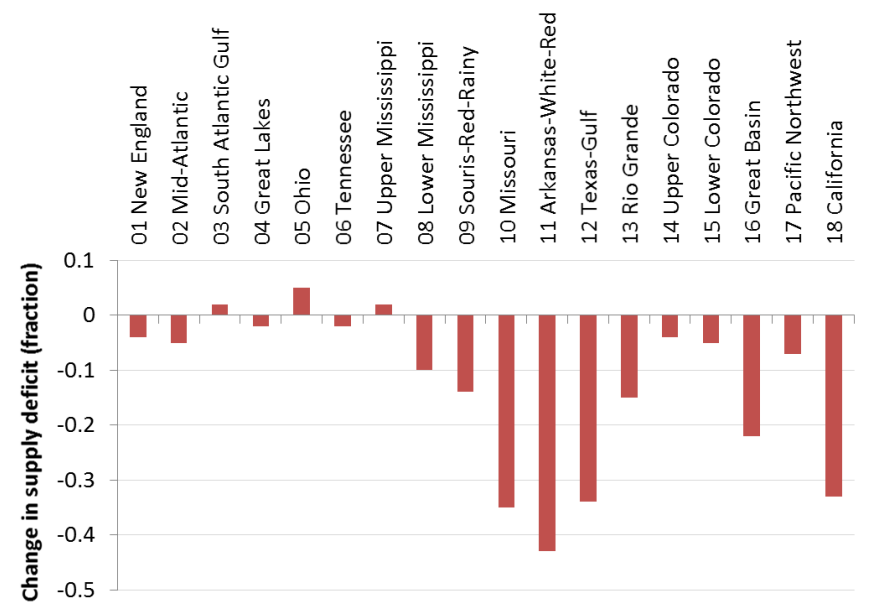

Figure 3. Relative change in ability of the integrated water model to meet the historical water demand when groundwater and return flow are considered in MOSART-WM. A decrease in historical supply deficit means an improvement in the ability of the integrated modeling framework to represent realistic water management.

Both groundwater use and return flow can redistribute water in space and consequently influence regional differences in water deficits. The combined effect of return flow and groundwater use could be two-fold: return flow changes the availability of local water to provide for withdrawals instead of consumptive demand in grid cells that are too far from the streams to be supported by reservoirs and cannot benefit from the reservoir's supply return flow as additional local supply. The withdrawals used as part of the return flow can add stress to the surface-water system, where the ratio of consumptive demand over withdrawals is small and where reservoir storage is low, i.e., the eastern US (Figure 2a,b). Including groundwater use allows more of the total demand (both consumptive and withdrawal) to be met so it may lower the relative deficit with respect to the benchmark. Different processes might dominate the spatial redistributions of water resources in different regions. The impacts of groundwater use and return flow can be evaluated by comparing the spatial patterns of various hydrologic aspects in the benchmark simulation and three numerical experiments.

Figure 4 presents the regulated flow simulated with the benchmark (WM), and the relative difference (ratio) in regulated flow due to redistribution of water from sectoral water management with return flow of surface water only (WM_return), changes in water storage due to the addition of groundwater as a source of supply (WM_GW), and the combined effects of return flow and groundwater supply (WM_GW_return). An east-west contrast emerged in the hydrologic pattern of the return flow dynamics (Figure 4b). Over the eastern US where the ratio of consumptive over withdrawal demand is the lowest (Figure 2b), the potential for recycling is high and the regulated flow tends to be either maintained (yellow) or increased (green to blue). As explained next with the pattern of supply deficit (Figure 5), the large surface withdrawals in the eastern US cannot always be met and consequently less consumptive demand is met and removed from the system, resulting in little recycling and more water in the streams

and grid cells. Because there is little storage capacity over the East, there is little opportunity to store and redistribute the increased flow into downstream grid cells. In reality, prorationing over the western US is based on a priority system with senior and junior water rights even if senior water rights are located downstream of junior water rights (Prior Appropriation). Over the eastern US, the Riparian Rights are applied and allow upstream users to use water on their properties as needed. In our modeling framework, the allocation from local streams follows the Riparian Rights while the allocation of remaining demand to reservoirs tends to even out the appropriation over all grid cells.

Over the Midwest and western US, the potential for reclaiming is low as the differences between withdrawals and consumptive demands are low. Over the Midwest, the large downstream irrigation projects in southern Colorado, southern California and Central Valley, Columbia River Basin Project and Snake River Basin, local water flow tends to become higher with return flow because the higher withdrawals can be met by upstream reservoirs and local streams. The streams are, however, drier until they reach large-capacity reservoirs (Garrison over the Missouri, for example) or the outlet (Colorado, California). Moreover, since WM_GW allocates water demand to surface and groundwater systems, this results in an increase in regulated flow in places where groundwater supply can be used and in the downstream rivers (Figure 4c). Over northern Texas, Arkansas, Red River, and lower Missouri, the main river flow enhancement due to groundwater is above 50% locally and it continues down to the river outlet, though with a lower factor. The combined effects of return flow and groundwater source (Figure4d) induce an increase in the overall flow. Spatial differences are notable where groundwater is the main source of supply and downstream of the region that is fed by the return flow (Figure 4c). Overall, the hydrological pattern induced by the return flow is more pronounced than the hydrological pattern induced by groundwater use.

Figure 5 shows the average daily deficit for the benchmark simulation and the absolute difference in unmet consumptive demand between the three experiments and the benchmark. For experiments WM_return and WM_GW_return, the unmet withdrawal demand was adjusted to reflect the unmet consumptive demand by simply conserving the ratio of met over total demand. Thus, all panels are in units of consumptive demand for proper evaluation. Comparing the return flow experiment with the benchmark (Figure 5a and 5b) highlights the east-west pattern shown earlier by the change in regulated flow. Over the East, we note the higher stress resulting in constrained withdrawals and therefore increased supply deficit but higher flow (Figure 4b). Over the Great Plains and western US, two types of patterns emerged. The first (yellow to blue or blue only) represents the reclaiming of the return flow in which the supply deficit is either maintained (yellow) or decreased (blue). This is feasible since the demand can be met in the first place due to the large storage capacity on which the grid cells rely for water supply. The second pattern is a red-to-blue transition that corresponds to a higher deficit upstream due to higher demands that cannot be met. Also the storage capacity can aggregate the unused water and redistribute it in space to its dependent grid cells and decrease their supply deficit (blue). This spatial redistribution is possible again due to the larger storage capacities. The east-west pattern due to return flow reflects a combination of the difference between withdrawals and consumptive demands, and storage capacity.

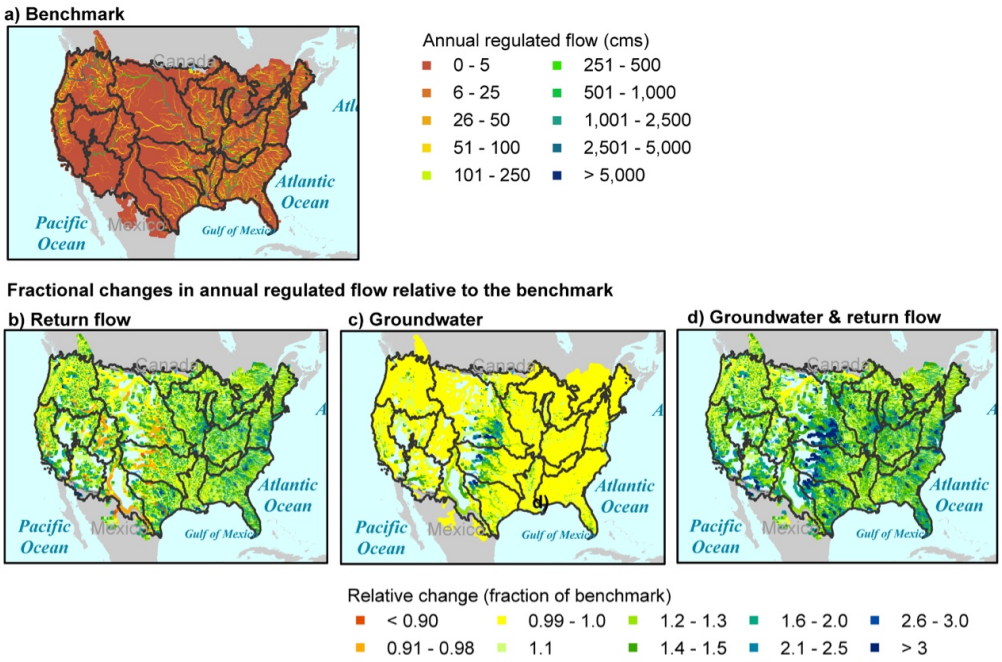

Figure 4. (a) Benchmark mean annual regulated flow in cubic meter per second. The second row shows the fractional change in regulated flow with respect to the benchmark for experiments including (b) return flow, (c) groundwater, and (d) both. Yellow indicates no change, green to blue indicates increased flow, and orange to red indicates drying.

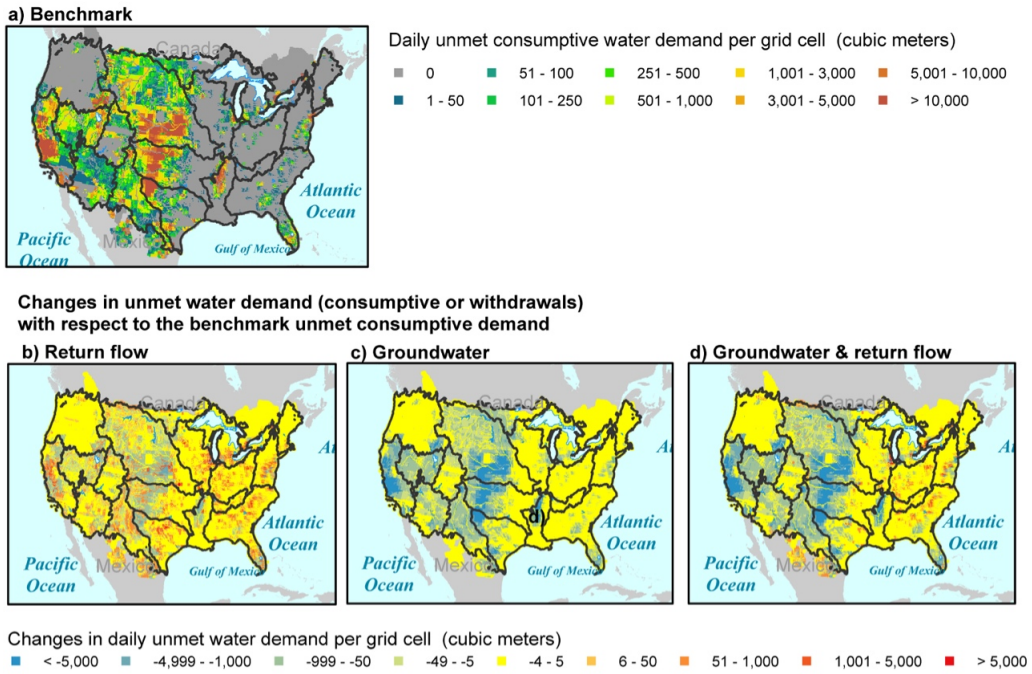

Figure 5. (a) Benchmark mean annual deficit in cubic meter per day. The second row shows the absolute change in supply deficit with respect to the benchmark for experiments using (b) return flow, (c) groundwater, and (d) both. Yellow indicates no change, green to blue indicates decrease in deficit, and orange to red indicates increase in deficit.

In summary, the MOSART-WM integrated water model has been extended with representation of groundwater use and return flow to improve modeling of water management. Using supply deficit as a metric for how well water management is represented by the model, it was demonstrated that including groundwater use and return flow improves the realism of water management by reducing supply deficit across almost all major river basins in the US (Figure 4). Using numerical experiments with and without groundwater use and return flow individually and in combination, the impacts of groundwater use and return flow have been investigated by comparing the spatial patterns of regulated flow and supply deficit among the simulations. Results show that spatial distribution of sectoral human activities associated with groundwater extractions and water use recycling have pronounced effects on the spatial patterns on streamflows (Figure 5) and water deficits (Figure 6). Such effects may induce feedbacks to regional climate through changes in evapotranspiration from irrigation and enhance the capacity of Earth system models to better capture the consequences of human water use activities on other Earth system components. Despite the relatively simple representation of groundwater and return flow, it was demonstrated that sectoral water management has important effects on differentiating water stress spatially because of the lower consumptive-over-withdrawal demand ratio for non-irrigation activities. The east-west variation in sectoral uses and associated spatial variations in the ratios of consumptive over withdrawal demand, combined with differences in reservoir storage capacity, create a clear east-west differentiation in water resources recycling. These findings emphasize the need for accurate parameterization of return flow, specifically linked to the sectoral and spatial variability in consumptive-over-withdrawal demand ratios, for accurate representation of water resources recycling, which is important for simulating water stress and the impacts of water use on the regional and global water cycles.

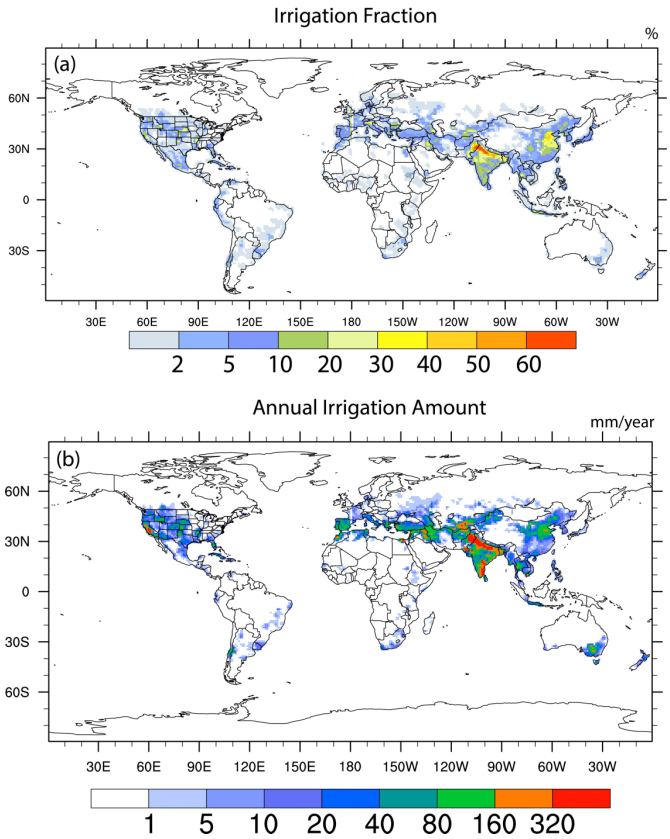

Figure 6. Global distribution of (a) irrigation fraction used as input to ALM-MOSART-WM and (b) irrigation demand simulated by ALM-MOSART-WM averaged over 1972-2004 simulated.

3.5 Modeling irrigation effects using the one-way coupled ALM-MOSART-WM model

Parallel to the new development with the offline implementation of MOSART-WM, the integrated water model has been coupled to ALM for ACME to represent interactions between irrigation and water management and improve consistency across the modeling components for water conservation, which is critical in global coupled simulations. To demonstrate successful one-way coupling of ALM with MOSART-WM, two simulations were performed for comparison. In the first simulation, surface-water irrigation is simulated in ALM assuming all demand is met but no water management. The simulated streamflow thus represents the natural flow conditions in rivers with no regulations. In the second simulation, surface-water demand is also simulated in ALM assuming all demand is met, but water demand can be met by local runoff as well as streams and reservoirs simulated by MOSART-WM with one-way coupling to ALM as described in the product documentation. The simulated streamflow represents regulated flow driven by irrigation water demand. In these simulations, ALM was configured following Leng et al. (2017) at 1-degree resolution globally using the spectral element grid of the ACME atmosphere model (ne30), while MOSART-WM was configured at 0.5-degree globally using a regular latitude/longitude grid, as in Li et al. (2015). Simulations were performed using observed atmospheric forcing [Qian et al. 2006] for 1972-2004. As crops are included in these simulations based on Drewniak et al. [2013], the carbon and nitrogen cycles of ALM are also included to simulated crop growth and the impacts of fertilization.

Figure 6a shows the global distribution of irrigation fraction (i.e., fractional area with irrigated crops) based on Portmann et al. [2010]. Areas with higher irrigation fraction are located in India, northern China, and the central and western US. The simulated irrigation demand is shown in Figure 6b. As expected, the irrigation demand is highest in areas with larger irrigation fraction. Reservoir operations are simulated by MOSART-WM to account for water allocation to meet the irrigation demand.

Figure 7 compares the streamflow in simulations with (WM) and without (natural) water management at Oroville and Hoover in the US where the dams regulate streamflow in part to supply for irrigation water demand. The Oroville Dam, the tallest in the US at 235 m, impounds Lake Oroville, fed by the Feather River, to provide irrigation in the San Joaquin valley. The Hoover Dam impounds Lake Mead, which is fed by the Colorado River and is the largest reservoir in the US by volume. At both locations, the natural flow has a strong seasonal cycle showing a large spring peak associated with snowmelt from the Sierra Nevada and Rocky Mountains, respectively. As irrigation demand is highest during summer, streamflow is regulated to produce a summer peak. The flow regulation is also reflected in the reservoir levels shown in Figure 8. At both Oroville and Hoover, the reservoir storage increases from January to April/May by impoundment. Beginning in May/June, the dams release water for irrigation so there is a simultaneous decrease in reservoir levels with the increase in flow.

Efforts are ongoing to improve the coupled ALM-MOSART-WM framework by including groundwater supply, which can be simulated by ALM using the groundwater pumping developed by Leng et al. (2014), and implementing two-way coupling of ALM with MOSART-WM to constrain irrigation water supply by water available in the main channels and reservoirs. In addition to offline ALM-MOSART-WM simulations driven by observed atmospheric forcing, simulations will be performed with ALM-MOSART-WM coupled to the ACME atmosphere model to evaluate the impacts of irrigation on precipitation through land-atmosphere interactions. The capability to represent human activities such as

irrigation and non-irrigation water demand and water management in ACME is important for understanding water-cycle changes due to perturbations of the Earth system.

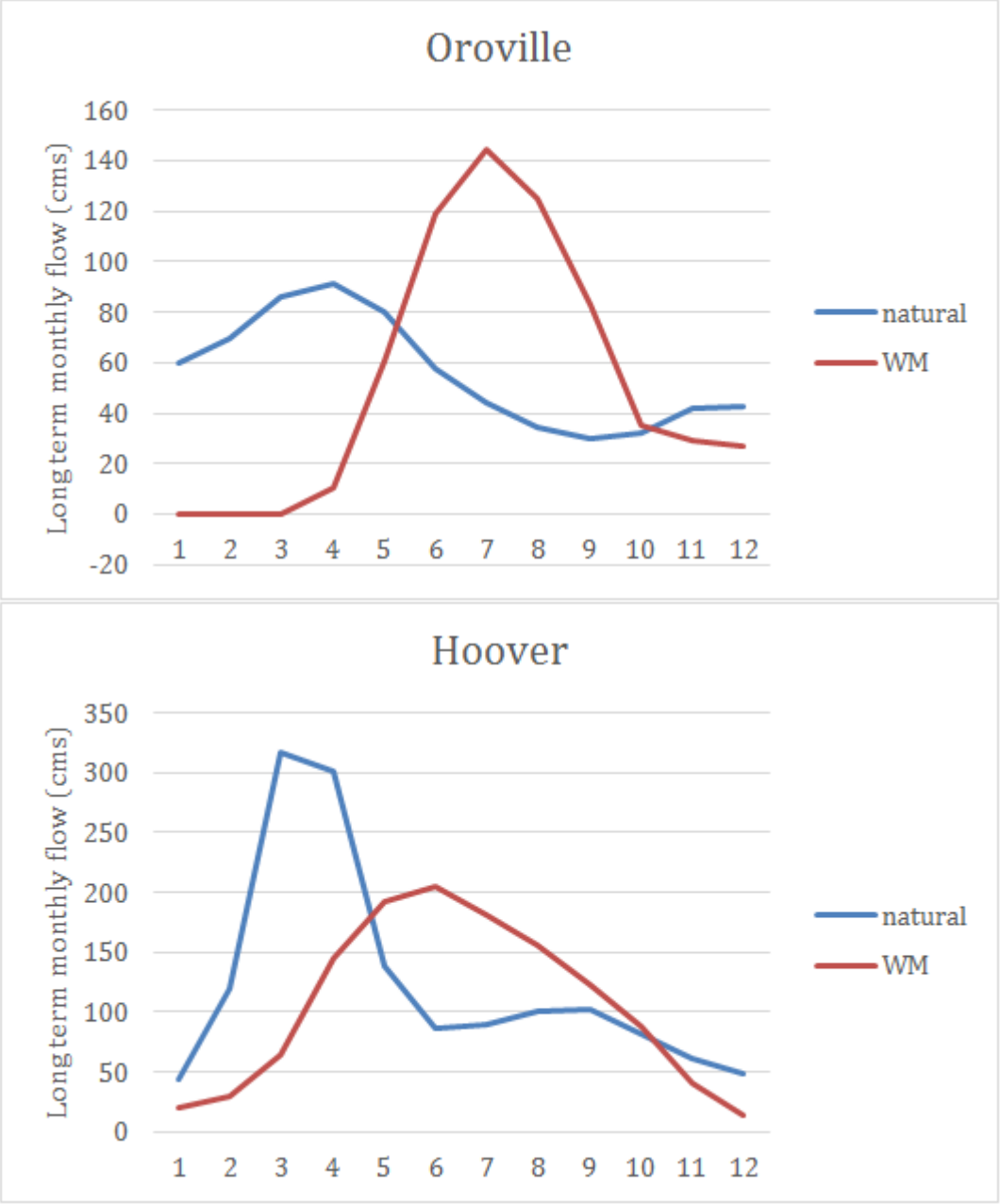

Figure 7. Long-term monthly mean streamflow (in cubic meter per second) simulated by ALM-MOSART-WM with (WM - red) and without (natural - blue) water management.

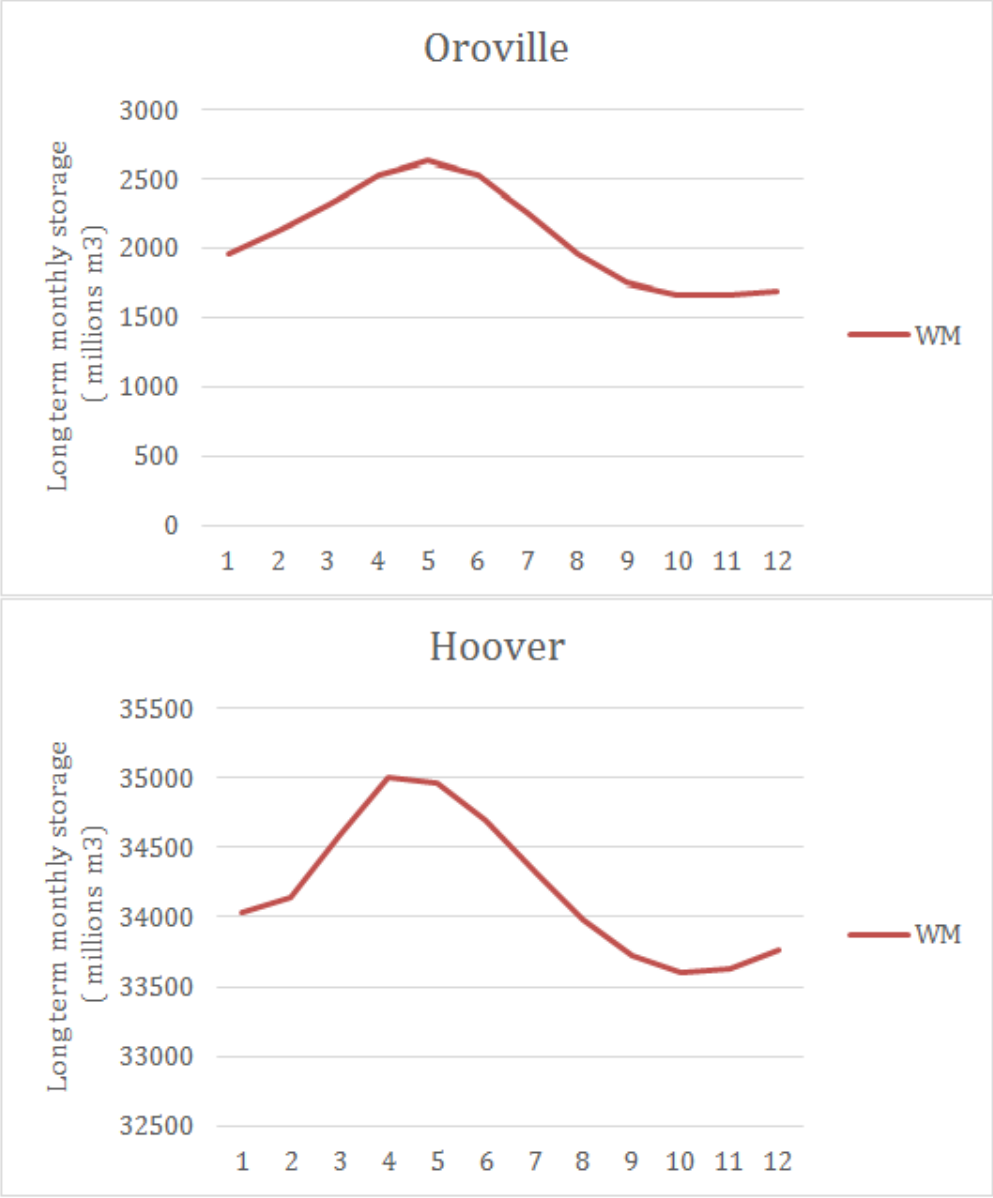

Figure 8. Long-term monthly mean reservoir storage (millions cubic meter) simulated by ALM-MOSART-WM with water management (WM – red). Note the significant difference in storage by the Oroville and Hoover dams.

4.0 References

Biemans, H., I. Haddeland, P. Kabat, F. Ludwig, R.W.A. Hutjes, J. Heinke, W. von Bloh, D. Gerten (2011), Impact of reservoirs on river discharge and irrigation water supply during the 20th century, *Water Resources Research*, 47, W03509.

Döll, P. (2009), Vulnerability to the impact of climate change on renewable groundwater resources: a global-scale assessment, *Environmental Research Letters*, *4*(3), 035006.

Döll, P., H. Hoffmann-Dobrev, F. T. Portmann, S. Siebert, A. Eicker, M. Rodell, G. Strassberg, and B. Scanlon (2012), Impact of water withdrawals from groundwater and surface water on continental water storage variations, *J. Geodyn*., 59–60, 143–56, doi:10.1016/j.jog.2011.05.001.

Drewniak, B., J. Song, J. Prell, V. Kotamarthi, and R. Jacob (2013), Modeling agriculture in the community land model, *Geoscientific Model Development*, *6*(2), 495-515.

Hejazi, M.I., N. Voisin, L. Liu, L. Bramer, D. Fortin, M. Huang, J. Hathaway, P. Kyle, L.R. Leung, H.Y. Li, Y. Liu, P. Patel, T. Pulsipher, J. Rice, T. Tesfa, C. Vernon, Y. Zhou (2015), 21st century US emissions mitigation increases water stress more than the climate change it is mitigating, *Proceedings of the National Academy of Sciences*, 112(34):10635-10640, doi:10.1073/pnas.1421675112.

Kenny, J. F., N.L. Barber, S.S. Hutson, K.S. Linsey, J.K. Lovelace, M.A. Maupin (2009) Estimated use of water in the United States in 2005, *U.S. Geological Survey Report*, Circular 1344, 52p, http://water.usgs.gov/watuse/.

Leng, G., M. Huang, Q. Tang, W.J. Sacks, H. Lei, and L.Y.R. Leung (2013), Modeling the Effects of Irrigation on Land Surface Fluxes and States over the Conterminous United States: Sensitivity to Input Data and Model Parameters, *Journal of Geophysical Research. D. (Atmospheres)*, 118(17):9789-9803, doi:10.1002/jgrd.50792.

Leng, G., M. Huang, Q. Tang, H. Gao, and L. R. Leung (2014), Modeling the effects of groundwater-fed irrigation on terrestrial hydrology over the conterminous United States, *J. Hydrometeorol.*, *15*(3), 957-972.

Leng, G., L. R. Leung, and M. Huang (2017), Significant impacts of irrigation water sources and methods on modeling irrigation effects in the ACME Land Model, *J. Adv. Mod. Earth Syst.*, doi: 10.1002/2016MS000885.

Li, H., M. S. Wigmosta, H. Wu, M. Huang, Y. Ke, A. M. Coleman, and L. R. Leung (2013), A physically based runoff routing model for land surface and earth system models, *J. Hydrometeorol.*, *14*(3), 808-828.

Li, H., L. R. Leung, A. Getirana, M. Huang, H. Wu, Y. Xu, J. Guo, and N. Voisin (2015), Evaluating global streamflow simulations by a physically based routing model coupled with the community land model, *J. Hydrometeorol.*, *16*(2), 948-971.

Liu L., M. Hejazi, P. Patel, P. Kyle, E. Davies, Y. Zhou, L. Clarke, and J. Edmonds (2015), Water Demands for Electricity Generation in the U.S.: Modeling Different Scenarios for the Water-Energy Nexus, *Technological Forecasting and Social Change*, in press, doi:10.1016/j.techfore.2014.11.004.

Pokhrel, Y. N., N. Hanasaki, P.J.-F. Yeh, T. Yamada, S. Kanae, and T. Oki (2012), Model Estimates of Sea Level Change due to Anthropogenic Impacts on Terrestrial Water Storage, *Nature Geoscience*, 5, 389-392, doi:10.1038/ngeo1476.

Postel, S., G.C. Daily, and P.R. Ehrlich (1996), Human Appropriation of Renewable Fresh Water. *Science*, 271 (February 9): 785-788.

Qian, T., A. Dai, K. E. Trenberth, and K. W. Oleson (2006), Simulation of global land surface conditions from 1948 to 2004. Part I: Forcing data and evaluations, J. Hydrometeorol., 7(5), 953-975.

Richey et al., (2015). Quantifying renewable groundwater stress with GRACE, *WRR*, 51(7), 5217-5238.

Portmann, F. T., S. Siebert, and P. Döll (2010), MIRCA2000—Global monthly irrigated and rainfed crop areas around the year 2000: A new high-resolution data set for agricultural and hydrological modeling, *Global Biogeochem. Cycles*, *24*(1).

Voisin, N., L. Liu, M. Hejazi, T. Tesfa, H. Li, M. Huang, Y. Liu, and L.R. Leung (2013a), One-way coupling of an integrated assessment model and a water resources model: evaluation and implications of future changes over the US Midwest, Hydrol. *Earth Syst. Sci.*, 17, 4555-4575, doi:10.5194/hess-17-4555-2013.

Voisin, N., H. Li, D. Ward, M. Huang, M. Wigmosta, and L.R. Leung, (2013b) On an improved sub-regional water resources management representation for integration into earth system models, *Hydrol. Earth Syst. Sci.*, 17, 3605-3622, doi:10.5194/hess-17-3605-2013.

Voisin, N., M. Hejazi, L.R. Leung, L. Liu, M. Huang, H.-Y. Li, and T. Tesfa (2017) Effects of spatially distributed sector water management on the redistribution of water resources in an integrated water model. *Water Resour. Res.*, *53*, 4253–4270, doi: 10.1002/2016WR019767.

Wada, Y., L. P. van Beek, C. M. van Kempen, J. W. Reckman, S. Vasak, and M. F. Bierkens (2010), Global depletion of groundwater resources, *Geophys. Res. Lett.*, *37*(20).

Wada, Y., L.P.H. vanBeek, F.C. Sperna Weiland, B.F. Chao, Y.-W. Wu, and M.F.P. Bierkens (2012), Past and future contribution of global groundwater depletion to sea-level rise, *Geophys. Res. Lett.*, 39, L09402, doi:10.1029/2012GL051230.

Wada, Y., D. Wisser, and M. Bierkens (2014), Global modeling of withdrawal, allocation and consumptive use of surface water and groundwater resources, *Earth System Dynamics*, *5*(1), 15.

U.S. DEPARTMENT OF
ENERGY

Office of Science